

Radiative corrections to the azimuthal asymmetry in transversely polarized Møller scattering

Lance Dixon* and Marc Schreiber†

Stanford Linear Accelerator Center, Stanford University, Stanford, California 94309, USA

(Received 27 February 2004; published 2 June 2004)

Experiment E158 at SLAC can measure an azimuthal asymmetry in single-spin, transversely polarized Møller scattering, $e^- \uparrow e^- \rightarrow e^- e^-$, which arises from a QED rescattering phase. We recompute the leading-order (one-loop) asymmetry, confirming previous results, and calculate the leading logarithmic QED corrections due to initial-state radiation from the beam and target electrons and due to final-state radiation. The size of these radiative corrections is quite sensitive to experimental details, such as the acceptance in energy and in polar angle of the scattered electron. For E158, the corrections are modest, increasing the parts-per-million asymmetry by roughly 1%.

DOI: 10.1103/PhysRevD.69.113001

PACS number(s): 12.20.Ds, 13.66.Lm, 13.88.+e

I. INTRODUCTION

Single-spin triple-product asymmetries, or asymmetries arising from transverse polarization, play a special role in scattering theory because they are directly sensitive to rescattering phases. An operator of the form $O \equiv \mathbf{S} \cdot (\mathbf{k} \times \mathbf{k}')$, where \mathbf{S} is a spin and \mathbf{k} and \mathbf{k}' are two different particle momenta, is odd under a “naive” time-reversal operation which reverses all spins and momenta, but does not exchange initial and final states. A nonzero value for O stems from terms in the covariant scattering amplitude that are proportional to the Levi-Civita tensor $\epsilon_{\mu\nu\rho\sigma}$, which always appears accompanied by a factor of i . Hence, in the absence of CP violation, a nonzero expectation value $\langle O \rangle$ requires an absorptive (imaginary) part for the amplitude, $\text{Im} T \neq 0$, which can be generated by rescattering—for example, by one-loop diagrams containing intermediate two-particle cuts.

There have been many theoretical and experimental studies of single-spin transversely polarized asymmetries in a variety of contexts. For instance, in the decay of a polarized neutron, $n^\uparrow \rightarrow p + e^- + \bar{\nu}_e$, an expectation value for $\mathbf{S}_n \cdot (\mathbf{k}_e \times \mathbf{k}_\nu)$ is produced by QED final-state interactions, which can therefore mask truly T -odd effects [1]. Analogous single-spin observables in the decay of a polarized Z boson to three hadronic jets, stemming from QCD and electroweak final-state interactions, have been studied theoretically [2] and bounded experimentally [3]. QCD final-state interactions can also play a role in generating azimuthal single-spin asymmetries in semi-inclusive pion leptonproduction off polarized protons at leading twist [4]. Similarly, a phase in the timelike electromagnetic proton form factor from QCD final-state interactions can be detected by measuring transverse proton polarization in the reaction $e^+ e^- \rightarrow p \bar{p}$ [5].

As a final example, QED rescattering phases produce an azimuthal asymmetry in the elastic scattering of electrons off transversely polarized protons, $ep^\uparrow \rightarrow ep$, or transverse final-state polarization in the time-reversed reaction $ep \rightarrow ep^\uparrow$. The QED asymmetry receives contributions not only from

two-photon exchange with a single proton in the intermediate state, but also from inelastic hadronic intermediate states; the latter terms are difficult to compute directly, although they can be bounded experimentally [6].

Perhaps the cleanest setting for studying such asymmetries is in a process dominated by QED, such as transversely polarized Møller scattering, $e^- \uparrow e^- \rightarrow e^- e^-$. Experiment E158 at SLAC performs Møller scattering of ≈ 45 GeV polarized electrons off unpolarized target electrons at rest. The prime goal of E158 is to measure the parity-violating right-left asymmetry in the cross section for longitudinal beam polarization, $A_{PV} = (\sigma_R - \sigma_L) / (\sigma_R + \sigma_L)$. The right-left asymmetry is sensitive to Z boson exchange and potentially to new physics, such as a new Z boson or contact interactions. The first measurement has yielded $A_{PV} = [-175 \pm 30(\text{stat.}) \pm 20(\text{syst.})] \times 10^{-9}$ [7]. While most of the E158 data were taken with the electron beam polarized longitudinally in order to accomplish this measurement, a fraction of the running was carried out with transverse electron polarization, enabling the measurement of an azimuthal asymmetry:

$$A_T(\phi) \equiv \frac{2\pi}{\sigma^\uparrow + \sigma^\downarrow} \frac{d(\sigma^\uparrow - \sigma^\downarrow)}{d\phi} \propto \mathbf{S}_e \cdot (\mathbf{k}_e \times \mathbf{k}'_e) \propto \sin \phi, \quad (1)$$

where \mathbf{S}_e is the spin of the incoming electron, with momentum \mathbf{k}_e , and ϕ is the azimuthal angle of the scattered electron (with momentum \mathbf{k}'_e) around the beam direction, measured from the direction of the transverse polarization.

In contrast to A_{PV} , a nonzero azimuthal asymmetry $A_T(\phi)$ can be generated by QED interactions alone. The calculation of $A_T(\phi)$ for transversely polarized Møller scattering at leading one-loop order was performed by Barut and Fronsda1 in 1960 [8] and by DeRaad and Ng in 1974 [9]. Because only the absorptive part of the scattering amplitude contributes to this observable, an s -channel cut is required. Hence only the box Feynman diagram enters, plus the version obtained by exchanging the two identical outgoing electron legs, as depicted in Fig. 1. Besides the rescattering phase, the effect requires an electron helicity flip. For center-of-mass (c.m.) energies much larger than the electron mass, $\sqrt{s} \gg m_e$, therefore, it takes the form $A_T(\phi)$

*Email address: lance@slac.stanford.edu

†Email address: mschreib@slac.stanford.edu

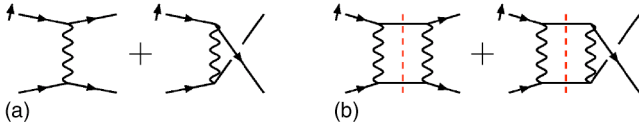


FIG. 1. (a) Tree-level graphs for electron-electron scattering. (b) One-loop graphs contributing to the azimuthal asymmetry for transverse polarization. Because an absorptive part in the s channel is required (the cut is indicated by the dashed line), only box diagrams contribute. The transverse spin of the beam electron is indicated by the arrow next to that incoming line.

$=\alpha\times m_e/\sqrt{s}\times f(\theta)\sin\phi$, where α is the fine structure constant, ϕ and θ are, respectively, the azimuthal and (c.m. frame) polar scattering angles, and f is a function of θ .

Since there are two identical electrons in the final state, $f(\theta)$ must be odd under $\theta\rightarrow\pi-\theta$; that is, a symmetric acceptance in θ (in an unsegmented detector) will wash out the asymmetry in ϕ . The E158 detector is well segmented in ϕ (12-fold), but coarsely segmented in θ (only 2-fold). Fortunately, the θ acceptance is almost entirely in the backward hemisphere in the c.m. frame, leaving the sensitivity of E158 to $A_T(\phi)$ quite high.

The E158 c.m. energy is roughly 200 MeV, so the asymmetry is of order $\alpha m_e/\sqrt{s}\sim 10^{-5}$. This may seem small, but it is two orders of magnitude larger than the electroweak asymmetry A_{PV} . Even though only a relatively small fraction of the data was taken with transversely polarized electrons, a precision of the order of a few percent can be achieved for $A_T(\phi)$. One can either test QED at this level or reverse the logic and use the QED prediction as a detector calibration or polarimeter [10].

At the percent level of precision, it becomes important to investigate the next-to-leading order (NLO), or $\mathcal{O}(\alpha^2)$, QED radiative corrections to $A_T(\phi)$. The full $\mathcal{O}(\alpha^2)$ calculation of the asymmetry requires two-loop scattering amplitudes for $e^{-\uparrow}e^{-}\rightarrow e^{-}e^{-}$ and one-loop scattering amplitudes for $e^{-\uparrow}e^{-}\rightarrow e^{-}e^{-}\gamma$. For $\sqrt{s}\gg m_e$, as in E158 kinematics, it would suffice to compute these amplitudes in the limit where one takes $m_e\rightarrow 0$ after extracting the leading m_e/\sqrt{s} behavior from the diagrams. This computation should be feasible, because it is known how to perform all the relevant two-loop four-point integrals [11] and one-loop five-point integrals [12] in this limit in dimensional regularization. (Similar amplitudes without transverse polarization have already been computed [13].)

In the present paper, we calculate the largest of the $\mathcal{O}(\alpha^2)$ corrections—those that are enhanced by the large logarithm $\ln(s/m_e^2)$ due to collinear singularities in initial-state radiation from both the incoming beam electron and the target electron, as well as final-state radiation. The amplitude for $e^{-\uparrow}e^{-}\rightarrow e^{-}e^{-}\gamma$ factorizes in these collinear limits, so that its full kinematic dependence is not required. In an electron structure function approach [14], analogues of the Dokshitzer-Gribov-Lipatov-Altarelli-Parisi (DGLAP) splitting kernels [15] enter our computation. In the case of target radiation and final-state radiation, only the unpolarized kernels are required. However, the radiation from the trans-

versely polarized beam electron also involves analogues of kernels for the evolution of transversely polarized quark distributions [16]. These kernels can be obtained from the standard longitudinally polarized splitting amplitudes by a change of basis.

We find that the magnitude of the leading-logarithmic NLO corrections is quite sensitive to the experimental cuts. Initial-state radiation (ISR), for example, lowers the effective value of s , which could enhance the asymmetry, since the leading-order asymmetry is proportional to m_e/\sqrt{s} . More importantly, ISR also skews the relation between polar angles in the post-radiation $e^{-}e^{-}$ c.m. frame and the laboratory frame, changing the effective c.m. polar angle acceptance of the experiment. Final-state radiation (FSR) does not have either of these properties and typically produces smaller corrections to the asymmetry.

This paper is organized as follows. In Sec. II we establish our notation and review the leading-order azimuthal asymmetry prediction [8,9]. In Sec. III we describe the leading-logarithmic NLO corrections and present numerical results for an experimental arrangement similar to E158. In Sec. IV we present our conclusions. In the Appendix we give a derivation of the kernel needed for evolution of the transversely polarized electron distribution.

II. NOTATION AND LEADING-ORDER RESULTS

We consider the process

$$e^{-\uparrow}(k_1)+e^{-}(k_2)\rightarrow e^{-}(k'_1)+e^{-}(k'_2)[+\gamma(k_\gamma)], \quad (2)$$

where the photon is only present at next-to-leading order. We use a right-handed xyz coordinate system, writing momenta $k^\mu=(k_t,k_x,k_y,k_z)$. We take the energy of the beam electron in the laboratory frame to be E and its momentum to be in the z direction: $k_1=(E,0,0,\sqrt{E^2-m_e^2})$. We let its polarization be in the positive x direction. In the laboratory frame, the unpolarized target electron is at rest, $k_2=(m_e,0,0,0)$. The momentum of the detected scattered electron is $k'_1=(E_{\text{lab}},\sqrt{E_{\text{lab}}^2-m_e^2}\sin\theta_{\text{lab}}\cos\phi,\sqrt{E_{\text{lab}}^2-m_e^2}\sin\theta_{\text{lab}}\sin\phi,\sqrt{E_{\text{lab}}^2-m_e^2}\cos\theta_{\text{lab}})$; its azimuthal angle ϕ increases from 0 in the positive x direction through $\pi/2$ in the positive y direction.

The Born-level differential cross section for Møller scattering, from the tree diagrams in Fig. 1a, is

$$\begin{aligned} \left.\frac{d\sigma^{\text{Born}}}{d\Omega}\right|_{\text{exact}} &= \frac{\alpha^2}{2s} \cdot \frac{(t^2+tu+u^2)^2+4m_e^2(m_e^2-t-u)(t^2-tu+u^2)}{t^2u^2}, \end{aligned} \quad (3)$$

where $s=(k_1+k_2)^2=2m_e(E+m_e)$, $u=(k'_1-k_2)^2=-2m_e(E_{\text{lab}}-m_e)$, $t=(k'_1-k_1)^2=4m_e^2-s-u$. (We include the statistical factor of 1/2 for identical electrons in

$d\sigma/d\Omega$, so such expressions should be integrated over two-body phase space for nonidentical particles.)

The leading term in the cross section containing the azimuthal dependence arises at order α^3 from the interference between the tree diagrams in Fig. 1(a) and the box diagrams in Fig. 1(b). The ϕ dependence at this order is given by [8,9]

$$\begin{aligned} \left. \frac{d\sigma^\phi}{d\Omega} \right|_{\text{exact}} &= -\frac{\alpha^3 m_e}{8} \frac{1}{\sqrt{s}} \sin\theta \sin\phi \sqrt{1 - \frac{4m_e^2}{s}} \frac{1}{t^2 u^2} \\ &\times \left\{ 3(s - 4m_e^2) \left[t(u - s + 2m_e^2) \ln\left(\frac{-t}{s - 4m_e^2}\right) \right. \right. \\ &\left. \left. - u(t - s + 2m_e^2) \ln\left(\frac{-u}{s - 4m_e^2}\right) \right] - 2(t - u)tu \right\}. \end{aligned} \quad (4)$$

We have reproduced this result independently.

Equations (3) and (4) include the exact dependence on the electron mass. However, in computing the NLO leading logarithms in s/m_e^2 , we shall drop the terms suppressed by powers of m_e^2/s in the leading-order asymmetry. The error induced by omitting these terms, for E158 kinematics, is much smaller than the size of the $\mathcal{O}(\alpha^2 \ln(s/m_e^2))$ corrections. The Born-level and leading ϕ -dependent cross sections then become

$$\frac{d\sigma^{\text{Born}}}{d\Omega} = \frac{\alpha^2}{2s} \left(\frac{t^2 + tu + u^2}{tu} \right)^2, \quad (5)$$

$$\begin{aligned} \frac{d\sigma^\phi}{d\Omega} &= -\frac{\alpha^3 m_e}{8} \frac{1}{\sqrt{s}} \sin\theta \sin\phi \frac{1}{t^2 u^2} \\ &\times \left\{ 3s \left[t(u - s) \ln\left(\frac{-t}{s}\right) - u(t - s) \ln\left(\frac{-u}{s}\right) \right] \right. \\ &\left. - 2(t - u)tu \right\}, \end{aligned} \quad (6)$$

and the kinematics can be simplified to

$$s = 2m_e E, \quad t = -2EE_{\text{lab}}(1 - \cos\theta_{\text{lab}}) = -\frac{s}{2}(1 - \cos\theta),$$

$$u = -2m_e E_{\text{lab}} = -\frac{s}{2}(1 + \cos\theta), \quad (7)$$

$$E_{\text{lab}} = \frac{E}{2}(1 + \cos\theta), \quad \cos\theta_{\text{lab}} = 1 - \frac{m_e}{E} \frac{1 - \cos\theta}{1 + \cos\theta}, \quad (8)$$

with θ the c.m. frame polar scattering angle.

Writing the asymmetry as

$$A_T(\phi) \equiv \frac{2\pi}{\sigma^\uparrow + \sigma^\downarrow} \frac{d(\sigma^\uparrow - \sigma^\downarrow)}{d\phi} \equiv \alpha_T \sin\phi, \quad (9)$$

Leading-order Azimuthal Asymmetry Coefficient

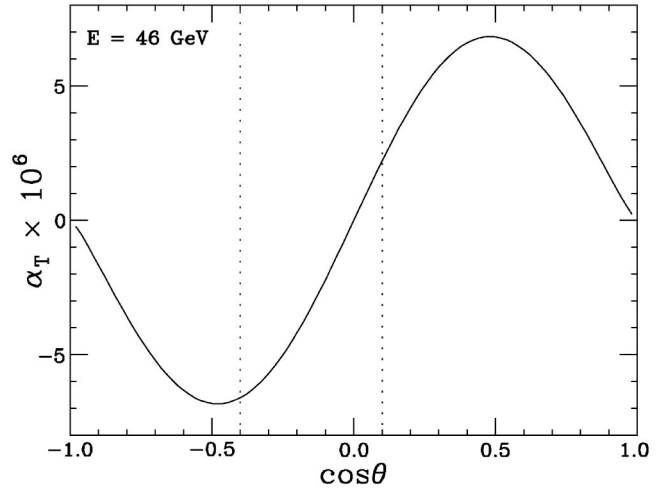


FIG. 2. The azimuthal asymmetry coefficient at leading order, α_T^{LO} , as a function of $\cos\theta$, for $E=46$ GeV, $\sqrt{s} \approx 217$ MeV. The vertical dotted lines indicate the approximate acceptance of E158 for leading-order kinematics.

we have

$$\alpha_T^{LO} = \frac{1}{\sin\phi} \frac{d\sigma^\phi/d\Omega}{d\sigma^{\text{Born}}/d\Omega}. \quad (10)$$

In Fig. 2 the leading-order asymmetry coefficient α_T^{LO} is plotted as a function of c.m. polar angle $\cos\theta$ for a beam energy of $E=46$ GeV or $\sqrt{s} \approx 217$ MeV. We set $\alpha = \alpha(\sqrt{s}) = 1/135.9$ here. [E158 probes central scattering in the c.m. frame, with $|t|$ and $|u|$ ranging between $0.3s$ and s , so the difference between $\alpha(\sqrt{s})$ and $\alpha(\sqrt{|t|})$ or $\alpha(\sqrt{|u|})$ is negligible, less than 0.1%.] The asymmetry is of the order of parts per million at this energy.

Note that α_T^{LO} is odd under $\theta \leftrightarrow \pi - \theta$ or, equivalently, that Eq. (6) is odd under $t \leftrightarrow u$. This asymmetry is a consequence of having two identical electrons in the final state. In the c.m. frame, if one electron is at an angle (θ, ϕ) , the other (at leading order) is at $(\pi - \theta, \phi + \pi)$. Because $\sin\phi$ is odd under $\phi \leftrightarrow \phi + \pi$, the coefficient α_T^{LO} must be odd under $\theta \leftrightarrow \pi - \theta$. The odd behavior means that the integrated asymmetry seen by an experiment integrating over a range in $\cos\theta$ is quite sensitive to the precise acceptance. For example, a symmetric forward-backward acceptance in the c.m. frame leads to zero asymmetry at leading order. The E158 polar-angle acceptance [7], $4.4 \text{ mrad} < \theta_{\text{lab}} < 7.5 \text{ mrad}$, corresponds mainly to the backward c.m. hemisphere for leading-order kinematics, $-0.4 \leq \cos\theta \leq 0.1$, as indicated by the dotted lines in Fig. 2.

As mentioned in the Introduction, the sensitivity to the acceptance could lead to relatively large QED corrections from hard photon radiation, which skews the kinematics of the $e^-e^- \rightarrow e^-e^-$ subprocess. In the next section we investigate these corrections in more detail.

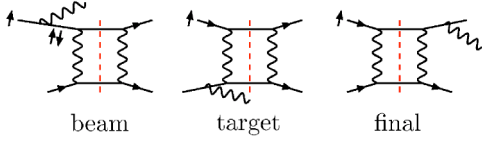


FIG. 3. Diagrams contributing to the NLO leading-logarithm-enhanced corrections to the azimuthal asymmetry. These graphs are to be interfered with corresponding graphs for the Born process. The exchange graphs are omitted. Also shown, with short arrows, are the transverse spin states of the initial electron and of the quasi-on-shell electron line in the case of beam radiation.

III. NLO CALCULATION AND RESULTS

The leading-logarithmic QED corrections to the azimuthal asymmetry arise from collinearly enhanced hard photon radiation. These contributions can be divided into beam (*b*), target (*t*), and final-state (*f*) radiation, according to the electron line with which the photon is collinear, as shown in Fig. 3. In each of these limits, the $e^-e^- \rightarrow e^-e^- \gamma$ cross section factorizes into a collinear splitting probability [14,15], multiplied by the lower-order $e^-e^- \rightarrow e^-e^-$ cross section evaluated for boosted kinematics. In the construction of the asymmetry, for the ϕ -dependent numerator the boosted cross section is provided by $d\sigma^\phi/d\Omega$ in Eq. (6); for the denominator of the asymmetry, it is $d\sigma^{\text{Born}}/d\Omega$ in Eq. (5). We still have to pay a factor of m_e/\sqrt{s} in $d\sigma^\phi/d\Omega$; hence we can neglect powers of m_e/\sqrt{s} in the splitting probabilities.

Although from the perspective of the laboratory frame one might not expect radiation off of the target to be important, in the center-of-mass frame such radiation is on an almost equal footing with radiation from the beam. One difference, though, is that we have to track the transverse polarization of the quasi-on-shell electron in the case of beam radiation, as indicated by the opposing transverse arrows in Fig. 3. A dilution of the transverse polarization will accompany the photon radiation in this case.

We let x denote the longitudinal momentum fraction retained by an incoming or outgoing electron, after it has radiated a collinear photon. The $x \rightarrow 1$ limit represents the emission of a soft photon. In the leading-logarithmic approximation, we neglect the transverse momentum of the photon in computing the boosted kinematics of the $e^-e^- \rightarrow e^-e^-$ subprocess. The integral over this small transverse momentum produces an overall factor of $\ln(s/m_e^2)$. The unpolarized splitting probability for massless electrons is well known [14]:

$$P(x) = \frac{1}{(1-x)_+} - \frac{1}{2}(1+x) + \frac{3}{4}\delta(1-x), \quad (11)$$

with the standard “plus” prescription definition

$$\int_0^1 dx \frac{f(x)}{(1-x)_+} \equiv \int_0^1 dx \frac{f(x) - f(1)}{1-x}. \quad (12)$$

For the case of radiation from the transversely polarized beam, we need to know the probability of a transverse spin flip. This probability is unsuppressed in the massless electron

limit, because a transverse polarization state is a coherent superposition of two different longitudinal (helicity) states. Thus a helicity flip is not required, only a different amplitude for the two different electron helicity configurations, for a given photon helicity. In the Appendix we perform this computation. The result can also be extracted from the QCD evolution equations for transversely polarized quarks [16] by converting color factors and coupling constants to the QED case:

$$P^{\uparrow\uparrow}(x) = \frac{1}{(1-x)_+} - \frac{1}{4}(3+x) + \frac{3}{4}\delta(1-x), \quad (13)$$

$$P^{\uparrow\downarrow}(x) = \frac{1}{4}(1-x), \quad (14)$$

where $P^{\uparrow\uparrow}$ ($P^{\uparrow\downarrow}$) is the splitting probability without (with) a transverse spin flip. These probabilities satisfy $P^{\uparrow\uparrow}(x) + P^{\uparrow\downarrow}(x) = P(x)$. It turns out that the $\delta(1-x)$ terms make a vanishing contribution to the azimuthal asymmetry, since they do not disrupt the leading-order kinematics, and the spin-flip probability vanishes in the soft limit $x \rightarrow 1$.

In the case of ISR, because the radiated photon carries momentum, the effective c.m. energy squared for the Møller scattering decreases from $s = 2m_e E$ to $s' = xs$. In the case of FSR, the radiation happens after the scattering, so $s' = s$. In radiative events, we use θ to denote the polar angle in the c.m. frame of the $e^-e^- \rightarrow e^-e^-$ subprocess. To take into account experimental cuts, we need to relate θ and x to the laboratory variables θ_{lab} and E_{lab} . The relations are

$$s' = xs, \quad E_{\text{lab}} = x \frac{E}{2}(1 + \cos \theta),$$

$$\cos \theta_{\text{lab}} = 1 - \frac{m_e}{xE} \frac{1 - \cos \theta}{1 + \cos \theta} \quad [\text{beam}], \quad (15)$$

$$s' = xs, \quad E_{\text{lab}} = \frac{E}{2}(1 + \cos \theta),$$

$$\cos \theta_{\text{lab}} = 1 - \frac{xm_e}{E} \frac{1 - \cos \theta}{1 + \cos \theta} \quad [\text{target}], \quad (16)$$

$$s' = s, \quad E_{\text{lab}} = x \frac{E}{2}(1 + \cos \theta),$$

$$\cos \theta_{\text{lab}} = 1 - \frac{m_e}{E} \frac{1 - \cos \theta}{1 + \cos \theta} \quad [\text{final}]. \quad (17)$$

We define a model experimental acceptance in the laboratory frame by

$$A: \quad E_{\text{lab}} > E_{\text{min}}, \quad \theta_{\text{min}} < \theta_{\text{lab}} < \theta_{\text{max}}. \quad (18)$$

Using Eqs. (15), (16), and (17) the acceptance A can be translated into acceptances A_b , A_t , and A_f bounding the integration region for x and θ in the respective correction

terms (and also the region A_0 which bounds the θ integral for leading-order, nonradiative events).

Including collinear radiation, the relevant terms in the differential cross section are modified as follows:

$$\frac{d\sigma^{\text{Bom}}(s)}{d\Omega} \rightarrow \frac{d\sigma^{\text{Bom}}(s)}{d\Omega} + \frac{\alpha}{\pi} \ln\left(\frac{s}{m_e^2}\right) \sum_{i=b,t,f} \int_0^1 dx P_i^{\text{Bom}}(x) \frac{d\sigma^{\text{Bom}}(s)}{d\Omega}, \quad (19)$$

$$\frac{d\sigma^\phi(s)}{d\Omega} \rightarrow \frac{d\sigma^\phi(s)}{d\Omega} + \frac{\alpha}{\pi} \ln\left(\frac{s}{m_e^2}\right) \sum_{i=b,t,f} \int_0^1 dx P_i^\phi(x) \frac{d\sigma^\phi(s)}{d\Omega}, \quad (20)$$

where $P_b^\phi = P^{\uparrow\uparrow}(x) - P^{\uparrow\downarrow}(x)$, $P_b^{\text{Bom}} = P_t^{\text{Bom}} = P_f^{\text{Bom}} = P_t^\phi = P_f^\phi = P(x)$. We insert Eqs. (19) and (20) into Eq. (10), perform the integrals over the respective acceptances in both the numerator and denominator of the asymmetry, and expand the result in α , thus obtaining, for the leading-logarithmic-corrected asymmetry coefficient,

$$\alpha_T^{LL} = \alpha_T^{LO} (1 + \delta_b + \delta_t + \delta_f), \quad (21)$$

where

$$\alpha_T^{LO} = \frac{N_0}{D_0}, \quad (22)$$

$$\delta_i = \frac{\alpha\sqrt{s}}{\pi} \ln\left(\frac{s}{m_e^2}\right) \left[\frac{N_i}{N_0} - \frac{D_i}{D_0} \right], \quad i=b,t,f. \quad (23)$$

Here the leading-order integrated results are

$$N_0 = \int_{A_0} d\cos\theta \frac{d\sigma^\phi(s)}{d\Omega}, \quad D_0 = \int_{A_0} d\cos\theta \frac{d\sigma^{\text{Bom}}(s)}{d\Omega}. \quad (24)$$

The radiative terms are

$$N_b = \int_{A_b} dx d\cos\theta [P^{\uparrow\uparrow}(x) - P^{\uparrow\downarrow}(x)] \frac{d\sigma^\phi(xs)}{d\Omega},$$

$$D_b = \int_{A_b} dx d\cos\theta P(x) \frac{d\sigma^{\text{Bom}}(xs)}{d\Omega}, \quad (25)$$

$$N_t = \int_{A_t} dx d\cos\theta P(x) \frac{d\sigma^\phi(xs)}{d\Omega},$$

$$D_t = \int_{A_t} dx d\cos\theta P(x) \frac{d\sigma^{\text{Bom}}(xs)}{d\Omega}, \quad (26)$$

TABLE I. Azimuthal asymmetry coefficient as a function of E_{\min} for $E=46$ GeV, $\theta_{\min}=4.4$ mrad, $\theta_{\max}=7.5$ mrad.

E_{\min} (GeV)	$\alpha_T^{LO} \times 10^6$	δ_b	δ_t	δ_f	$\alpha_T^{LL} \times 10^6$
8	-3.7949	-0.0221	0.0452	0.0011	-3.8826
10	-3.7949	-0.0121	0.0282	0.0015	-3.8562
12	-3.7949	-0.0060	0.0165	0.0019	-3.8348
14	-3.4180	-0.0040	0.0109	0.0022	-3.4414

$$N_f = \int_{A_f} dx d\cos\theta P(x) \frac{d\sigma^\phi(s)}{d\Omega},$$

$$D_f = \int_{A_f} dx d\cos\theta P(x) \frac{d\sigma^{\text{Bom}}(s)}{d\Omega}. \quad (27)$$

In Table I we present results for the azimuthal asymmetry coefficient for $E=46$ GeV as a function of the minimum accepted energy E_{\min} for $4.4 < \theta_{\text{lab}} < 7.5$ mrad. We give the leading-order result integrated over the acceptance, α_T^{LO} ; the beam, target, and final-state fractional corrections δ_b , δ_t , and δ_f ; and the QED-corrected result α_T^{LL} . The leading-order result does not depend on E_{\min} until $E_{\min} > 13$ GeV; at that point the E_{\min} cut starts to remove the most backward-scattered electrons (in the c.m. frame), which have the lowest energies in the laboratory frame. The corrections from beam and target radiation have opposite sign, because such radiated photons skew in opposite directions the relation between the subprocess c.m. frame and the laboratory frame, as indicated by Eqs. (15) and (16). For beam radiation, as x decreases from 1, a given angle in the subprocess c.m. frame boosts to a larger angle in the laboratory frame. Hence, for small x , the experimental cuts now sample some of the c.m. forward hemisphere, where the LO asymmetry is positive. Thus δ_b is negative. For target radiation, however, as x decreases from 1, the boost back to the laboratory frame becomes larger and the resulting c.m. angles boost to smaller laboratory frame angles. Now small x forces the experimental cuts to sample more of the c.m. backward hemisphere, where the LO asymmetry can be even more negative. Thus δ_t is positive. It is also larger in magnitude than δ_b , which may be due to the depolarization of the beam by ISR: $P^{\uparrow\uparrow}(x) - P^{\uparrow\downarrow}(x) < P(x)$. As E_{\min} decreases, both δ_b and δ_t increase in magnitude, as more hard radiative events are permitted, which skew the kinematics more. Final-state radiation does not alter the LO relation between θ and θ_{lab} . It only has an effect via the minimum energy cut, which affects the effective $\cos\theta$ acceptance through Eq. (17) for E_{lab} . Indeed, δ_f decreases as E_{\min} is lowered.

Table II presents azimuthal asymmetry results with the minimum accepted energy E_{\min} held fixed at 13 GeV and the minimum angle fixed at $\theta_{\min}=4.4$ mrad, but varying the maximum angle θ_{\max} . Now the variation in the QED-corrected result is dominated by the variation in the leading-order term α_T^{LO} , since the leading-order acceptance is changing. However, the size of δ_b and δ_t also depends strongly on θ_{\max} , presumably because the *slope* of the leading-order

TABLE II. Azimuthal asymmetry coefficient as a function of θ_{\max} for $E = 46$ GeV, $E_{\min} = 13$ GeV, $\theta_{\min} = 4.4$ mrad.

θ_{\max} (mrad)	$\alpha_T^{LO} \times 10^6$	δ_b	δ_t	δ_f	$\alpha_T^{LL} \times 10^6$
6.5	-2.6358	-0.0102	0.0241	0.0016	-2.6724
7.0	-3.2762	-0.0061	0.0166	0.0019	-3.3103
7.5	-3.7949	-0.0044	0.0121	0.0021	-3.8241
8.0	-3.8039	-0.0043	0.0120	0.0021	-3.8330

asymmetry at $\theta = \theta_{\max}$ (the left dotted line in Fig. 2) is also changing; the slope determines how effective the skewed kinematics are in altering the asymmetry.

IV. CONCLUSIONS AND OUTLOOK

In this paper we computed the leading-logarithmic QED corrections to the azimuthal symmetry in transversely polarized Møller scattering, which relies on a one-loop rescattering phase and is currently being measured by the E158 experiment. The correction term arising from radiation off the beam electron involves a transverse spin-flip splitting probability analogous to that encountered in the QCD evolution of transversely polarized quark distributions, which dilutes the beam polarization. The corrections from radiation off the beam and target are opposite in sign, because they skew the kinematic relation between the subprocess center-of-mass frame and laboratory frame in opposite directions. Final-state radiation is smaller in size. The net effect depends on the cuts, but is typically about a 1% increase in the magnitude of the asymmetry. This shift is somewhat below the anticipated precision of the E158 measurement of a few percent. In principle, therefore, the present QED prediction, combined with the E158 measurement, could be used as an alternate way to measure the beam polarization or calibrate the azimuthal response of the detector. Finally, computation of the nonlogarithmically enhanced QED corrections is a feasible future project, though probably not mandated by the presently achievable experimental precision.

ACKNOWLEDGMENTS

We thank Yury Kolomensky, Krishna Kumar, and Mike Woods for suggesting this problem and for helpful discussions and information about the E158 experiment. We are also grateful to Stan Brodsky and Michael Peskin for useful conversations and comments on the manuscript. This research was supported by the U.S. Department of Energy under contract DE-AC03-76SF00515.

APPENDIX: EVOLUTION OF TRANSVERSE ELECTRON POLARIZATION

Collinear photon radiation can produce a transverse spin flip for a massless electron because the transverse spin state is a coherent superposition of both longitudinal spin (helicity) states. There is no longitudinal spin flip in the massless limit, but for a given photon helicity, the amplitude for radiation depends on the electron helicity. In the transverse

basis, this dependence generates the spin flip.

Explicitly, the transverse states $|\uparrow\rangle$ and $|\downarrow\rangle$ are given in terms of longitudinal states $|+\rangle$ and $|-\rangle$ by

$$|\uparrow\rangle = \frac{1}{\sqrt{2}}(|+\rangle + |-\rangle), \quad |\downarrow\rangle = \frac{1}{\sqrt{2}}(|+\rangle - |-\rangle). \quad (\text{A1})$$

The x dependence of the amplitudes for collinear splitting, $e \rightarrow e\gamma$, in the helicity basis can be extracted from analogous results for the $q \rightarrow qg$ splitting amplitudes in QCD (see, e.g., Ref. [17]). The nonvanishing, helicity-conserving amplitudes are

$$\mathcal{A}(e^{(+)} \rightarrow e^{(+)}\gamma^{(+)}) = \mathcal{A}(e^{(-)} \rightarrow e^{(-)}\gamma^{(-)}) = \frac{1}{\sqrt{1-x}}, \quad (\text{A2})$$

$$\mathcal{A}(e^{(-)} \rightarrow e^{(-)}\gamma^{(+)}) = \mathcal{A}(e^{(+)} \rightarrow e^{(+)}\gamma^{(-)}) = \frac{x}{\sqrt{1-x}}. \quad (\text{A3})$$

The x dependence of the usual unpolarized splitting probability for $x < 1$, $P(x) \propto (1+x^2)/(1-x)$, can easily be recovered by summing the squares of these amplitudes. Here we wish to transform these amplitudes to the transverse electron spin basis (A1),

$$\begin{aligned} \mathcal{A}(e^\uparrow \rightarrow e^\uparrow\gamma^{(+)}) &= \frac{1}{\sqrt{2}}(1 \ 1) \begin{pmatrix} \frac{1}{\sqrt{1-x}} & 0 \\ 0 & \frac{x}{\sqrt{1-x}} \end{pmatrix} \frac{1}{\sqrt{2}} \begin{pmatrix} 1 \\ 1 \end{pmatrix} \\ &= \frac{1+x}{2\sqrt{1-x}}, \end{aligned} \quad (\text{A4})$$

$$\begin{aligned} \mathcal{A}(e^\uparrow \rightarrow e^\downarrow\gamma^{(+)}) &= \frac{1}{\sqrt{2}}(1 \ 1) \begin{pmatrix} \frac{1}{\sqrt{1-x}} & 0 \\ 0 & \frac{x}{\sqrt{1-x}} \end{pmatrix} \frac{1}{\sqrt{2}} \begin{pmatrix} 1 \\ -1 \end{pmatrix} \\ &= \frac{\sqrt{1-x}}{2}. \end{aligned} \quad (\text{A5})$$

The amplitudes for the case of negative photon helicity have the same magnitudes, using parity. Note that the relative phase of the amplitudes given in Eqs. (A2) and (A3) is important in Eqs. (A4) and (A5); it can be fixed by requiring that the amplitudes become independent of the electron helicity in the soft photon limit $x \rightarrow 1$.

The square of Eq. (A5) gives the x dependence of the transverse spin-flip splitting probability in Eq. (14), $P^{\uparrow\downarrow}(x)$

$= \frac{1}{4}(1-x)$. This term needs no plus-prescription regularization as $x \rightarrow 1$; nor is there a $\delta(1-x)$ term. The square of Eq. (A4) gives the x dependence of $P^{\uparrow\uparrow}(x)$ in Eq. (13); here, plus-prescription regularization is required. The overall nor-

malization of $P^{\uparrow\uparrow}$ and $P^{\uparrow\downarrow}$ can be fixed by requiring their sum to be equal to $P(x)$ in Eq. (11). The $\delta(1-x)$ term in $P^{\uparrow\uparrow}$ can be inferred from electron number conservation, $\int_0^1 dx P(x) = \int_0^1 dx [P^{\uparrow\uparrow}(x) + P^{\uparrow\downarrow}(x)] = 1$.

-
- [1] J.D. Jackson, S.B. Trieman, and H.W. Wyld, Jr., Phys. Rev. **106**, 517 (1957).
- [2] K. Fabricius, I. Schmitt, G. Kramer, and G. Schierholz, Phys. Rev. Lett. **45**, 867 (1980); J.G. Körner, G. Kramer, G. Schierholz, K. Fabricius, and I. Schmitt, Phys. Lett. **94B**, 207 (1980); A. Brandenburg, L.J. Dixon, and Y. Shadmi, Phys. Rev. D **53**, 1264 (1996); E. Maina, S. Moretti, and D.A. Ross, J. High Energy Phys. **04**, 056 (2003).
- [3] SLD Collaboration, K. Abe *et al.*, Phys. Rev. Lett. **75**, 4173 (1995); **86**, 962 (2001).
- [4] S.J. Brodsky, D.S. Hwang, and I. Schmidt, Phys. Lett. B **530**, 99 (2002).
- [5] A.Z. Dubnickova, S. Dubnicka, and M.P. Rekaló, Nuovo Cimento A **109**, 241 (1996); S. Rock, in *Proceedings of the e^+e^- Physics at Intermediate Energies Conference*, edited by D. Bettoni, eConf **C010430**, W14, 2001, hep-ex/0106084; S.J. Brodsky, C.E. Carlson, J.R. Hiller, and D.S. Hwang, Phys. Rev. D **69**, 054022 (2004).
- [6] R.N. Cahn and Y.S. Tsai, Phys. Rev. D **2**, 870 (1970); A.J.G. Hey, *ibid.* **3**, 1252 (1971); A. De Rújula, J.M. Kaplan, and E. De Rafael, Nucl. Phys. **B35**, 365 (1971); **B53**, 545 (1973); A. Afanasev, I. Akushevich, and N.P. Merenkov, hep-ph/0208260; T. Powell *et al.*, Phys. Rev. Lett. **24**, 753 (1970).
- [7] SLAC E158 Collaboration, P.L. Anthony *et al.*, Phys. Rev. Lett. **92**, 181602 (2004).
- [8] A.O. Barut and C. Fronsdal, Phys. Rev. **120**, 1871 (1960).
- [9] L.L. DeRaad, Jr. and Y.J. Ng, Phys. Rev. D **10**, 683 (1974); **10**, 3440 (1974); **11**, 1586 (1975).
- [10] SLAC E158 Collaboration, M. Woods, eConf. **C0307282**, TTH04, 2003, hep-ex/0403010.
- [11] V.A. Smirnov, Phys. Lett. B **460**, 397 (1999); V.A. Smirnov and O.L. Veretin, Nucl. Phys. **B566**, 469 (2000); C. Anastasiou, E.W.N. Glover, and C. Oleari, *ibid.* **B565**, 445 (2000); **B575**, 416 (2000); **B585**, 763(E) (2000); J.B. Tausk, Phys. Lett. B **469**, 225 (1999); C. Anastasiou, T. Gehrmann, C. Oleari, E. Remiddi, and J.B. Tausk, Nucl. Phys. **B580**, 577 (2000).
- [12] Z. Bern, L.J. Dixon, and D.A. Kosower, Nucl. Phys. **B412**, 751 (1994).
- [13] Z. Kunszt, A. Signer, and Z. Trócsányi, Phys. Lett. B **336**, 529 (1994); Z. Bern, L.J. Dixon, and A. Ghinculov, Phys. Rev. D **63**, 053007 (2001).
- [14] V.N. Baier, V.S. Fadin, and V.A. Khoze, Nucl. Phys. **B65**, 381 (1973); G. Montagna, F. Piccinini, and O. Nicrosini, Phys. Rev. D **48**, 1021 (1993).
- [15] V.N. Gribov and L.N. Lipatov, Yad. Fiz. **15**, 781 (1972) [Sov. J. Nucl. Phys. **15**, 438 (1972)]; G. Altarelli and G. Parisi, Nucl. Phys. **B126**, 298 (1977); Y.L. Dokshitzer, Zh. Éksp. Teor. Fiz. **73**, 1216 (1977) [Sov. Phys. JETP **46**, 641 (1977)].
- [16] X. Artru and M. Mekhfi, Z. Phys. C **45**, 669 (1990).
- [17] M.L. Mangano and S.J. Parke, Report No. FERMILAB-CONF-87-121-T, in Proceedings of the International Europhysics Conference on High Energy Physics, Uppsala, Sweden, 1987; Z. Bern, L.J. Dixon, D.C. Dunbar, and D.A. Kosower, Nucl. Phys. **B425**, 217 (1994).